minerals

MDPI

Article

Application of Depletion Attraction in Mineral Flotation: I. Theory

Junhyun Choi [1], Gahee Kim [1], Sowon Choi [1], KyuHan Kim [2], Yosep Han [1], Scott A. Bradford [3], Siyoung Q. Choi [4,*] and Hyunjung Kim [1,3,*]

1 Department of Mineral Resources and Energy Engineering, Chonbuk National University, 567 Baekje-daero, Deokjin-gu, Jeonju, Jeonbuk 54896, Korea; anar3092@naver.com (J.C.); pingki1222@naver.com (G.K.); thdnjs1015@naver.com (S.C.); yosep@jbnu.ac.kr (Y.H.)
2 Department of Chemical & Biomolecular Engineering, Seoul National University of Science & Technology, 232 Gongneung-ro, Nowon-gu, Seoul 01811, Korea; kyuhankim@seoultech.ac.kr
3 U.S. Salinity Laboratory, USDA, ARS, Riverside, CA 92507, USA; scott.bradford@ars.usda.gov
4 Department of Chemical and Biomolecular Engineering, Korea Advanced Institute of Science and Technology (KAIST), Daejeon 305-701, Korea
* Correspondence: sqchoi@kaist.ac.kr (S.Q.C.); kshjkim@jbnu.ac.kr (H.K.); Tel.: +82-42-350-4369 (S.Q.C.); +82-63-270-2370 (H.K.); Fax: +82-63-270-2366 (H.K.)

Received: 29 August 2018; Accepted: 30 September 2018; Published: 14 October 2018

Abstract: We investigate the role of depletion interactions in the particle–bubble interactions that determine the attachment capability of particles on the bubble surface in flotation. In this article, we propose a theoretical model that explains how this attractive interaction could enhance flotation efficiency. Two optimum conditions are determined for the concentration and molecular weight of the depletion agent. The optimum concentration can be determined through the extent of surface activity of the depletion agents. The magnitude of the depletion attraction increases as the concentration increases; however, an increase in the concentration simultaneously enhances its surface concentration. The bubble surface adsorption of the depletion agent results in polymer brushes on the bubble surface that produce a large repulsive interaction. In contrast, the optimal molecular weight of the depletion agents is given by the interaction between the depletion agent sizes, which is determined by its molecular weight and Debye length which is determined by the solution ionic strength. We demonstrate that exploiting this depletion interaction could significantly enhance the flotation efficiency and in principal could be used for any particle system.

Keywords: flotation; depletion attraction; particle-bubble interaction; depletion agent

1. Introduction

Flotation is a physico-chemical separation technique for particles and it has been used extensively for a wide range of mineral processes [1–5]. Although it is useful and powerful, flotation involves extremely complicated dynamic processes with various phase components (gas, liquid and solid) under flow; examples include the attachment of solid minerals to gas bubbles, the mixing of solid minerals under vigorous liquid flows, the formation of gas bubbles and the motion of bubbles due to buoyant force; none of which are completely understood. Furthermore, other components such as collectors and frothers are necessary addition [6–8] and the flows involved in this process are usually turbulent [9–11]. This complex problem is challenging to control thoroughly. Moreover, when encountering different systems, a strategy must be designed for each system because individual systems generally behave in distinct ways both qualitatively and quantitatively. Despite such complexity, researchers have made substantial efforts and progress along with some understanding of the mechanisms of flotation [12–15].

More specially, the understanding of the interaction between bubbles and minerals is crucial because it highly affected the flotation performance [12,16–19]. For these reasons, understanding how different minerals attach onto the bubbles is considered essential to improving the flotation technique.

Researchers have investigated numerous systems using a variety of techniques to improve the attachment of particles onto the bubbles [20–29]. For example, many previous studies have focused on imparting hydrophobicity to the surface because the hydrophobic surface of minerals favorably interacts with bubbles [2,21–23,30–32]. Therefore, the type and number of suitable collectors that can selectively recover the minerals have been investigated. Furthermore, other researchers have focused on the influence of electrolyte solutions as well as selective adsorption of collector on the mineral surface to regulate the interaction between the particles and bubbles [6,20,25,26,29]. The dissolved ions compress the electrical double layer (EDL) of the particles, which reduces the electrostatic repulsive force [6,33,34]. The EDL compression improves the attachment between the particles and bubbles, thus increasing the flotation efficiency.

As described above, most previous research has emphasized four basic interactions: electrostatic, van der Waals, hydrophobic and capillary interactions, which are considered to be crucial in colloid chemistry. The first three interactions do not appear till interacting particles reach certain separation distance and the interplay among these three interactions determines the energy barrier that decides whether minerals can reach the bubble surface. In contrast, the capillary interaction can only be applied when the mineral surfaces come into contact with the bubble surfaces. Until the bubble and mineral surfaces touch each other, the force does not exist; however, once the minerals are trapped at the bubble surface, they cannot escape in most situations due to the large capillary forces [35,36]. Thus, it is natural to ask whether other interactions provide a better tool to control the flotation process. One interaction that has not yet been investigated in the flotation community is the depletion interaction (sometimes also referred to as depletion attraction or osmotic pressure by depletion).

The depletion interaction is well known and has been widely used in colloid chemistry since the Asakura–Oosawa theory was first proposed in the 1950s [37]; the theory describes the presence of attractive force appearing between two bodies immersed in a solution of macromolecules and the magnitude varies with concentration, shape and charge of macromolecules. The depletion interaction is an entropic interaction that also occurs in a mixture of large colloids and small colloids [38–41]. Figure 1 presents a schematic of the depletion interaction. The small colloids provide the isotropic osmotic pressure when the large colloids are sufficiently separated; thus, the depletion force does not affect the interactions between large colloids. However, when their separation distance is closer than the size of the small colloids or the "excluded volume" is overlapped, the large particles are pushed toward each other via anisotropic osmotic pressure due to the exclusion of the small colloids between the large colloids. This force functions as an attractive interaction of the large colloids [37–39,41,42]. Through adding small colloids in a flotation system, the bubbles and mineral particles might behave as two large colloids in flotation. As a result, the attractive interaction via the depletion could enhance the attachment of mineral particles through overcoming preexisting energy barriers if the excluded volumes of the bubble surface and minerals overlap.

At the same time, these small colloids, which are referred to as depleting agents, can also adversely affect the attachment of minerals to the bubbles. Typically, neutral polymers such as polyethylene glycol, polyethylene oxide and dextran that are used as depleting agents can provide either attractive or repulsive interactions depending on whether they adsorb to the surface of larger colloids or are suspended in the solution; if they are freely suspended in the solution, they function as depleting agents, which yields attractive depletion interactions; in contrast, if they adhere to the surface of the large colloids, they function as polymer brushes, which results in steric repulsion [43–49]. These interesting properties of neutral water-soluble polymers could be exploited in the flotation process because they can be attached on both the bubble and mineral surfaces.

The goal of this paper, which is the first in a series of papers, is to understand the role of the depletion interaction theoretically when considering flotation. As mentioned above, it is difficult

to consider all interactions involved in flotation together but this problem is countered through considering each interaction with the depletion attraction. Furthermore, this investigation structure provides a rational direction on how to exploit the depletion interaction so that the flotation efficiency can be increased. We analyze this complicated process in the simplest terms for the depletion interaction and only interactions between the bubbles and target particles are considered.

In the following sections, we examine how the depletion interaction affects the overall interaction between the bubbles and minerals and also how much the attachment behavior is improved. We begin with a model similar to the Smoluchowski equation of colloidal aggregation in order to compute the probability of minerals to attach onto the bubbles depending on the interaction energy. First, using the well-known Derjaguin–Landau–Verwey–Overbeek (DLVO) theory, we consider the influence of the bubble-particle attachment interaction on two major interaction parameters (electrostatic and van der Waals interactions) and then, the depletion interaction was additionally added as a function of the depletant concentrations. We also demonstrate that when the depleting agents are surface active, they can function as polymer brushes at the bubble surface, thus providing a repulsive interaction. Second, we discuss how the molecular weights of the depletion agents affect the flotation efficiency and explain its relationship with the ionic strengths of solutions. Finally, we examine the depletion interaction strength compared to the gravitational force and capillary force.

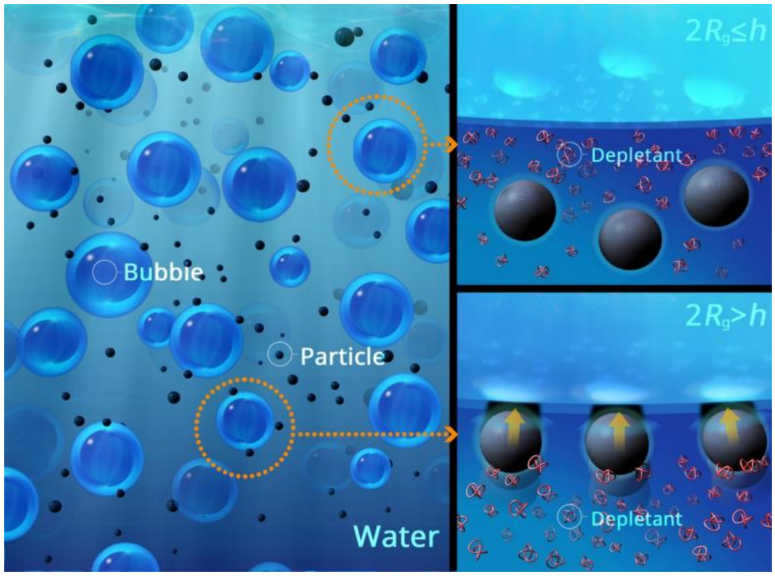

Figure 1. Schematic of the depletion interaction in a typical flotation process. The depletion agent does not influence the particle-bubble interaction when their separation distance (h) is larger than the diameter of the depletion agent ($2R_g$), that is, $h \geq 2R_g$. However, the attractive force due to depletion begins to be exerted when the particles come closer to the bubble than the diameter of the depletion agent ($h < 2R_g$).

2. Theoretical Background

2.1. Probability for Particles to Attach to Bubbles Without Convective Flow

We begin with the flux of particles from the bulk to the surface. For simplicity, we assume that a convective flow does not exist in the system and that the only route for particles to reach the bubble surface is via diffusion based on Abrahamson approach [10,50,51]. Although particles in flotation are typically non-Brownian particles with sizes larger than 10 μm, this theory remains valid because we only look for how much energy is required to obtain particle flux. The actual driving force of this flux

in a real system is the fluid flow; however, this is ignored at this stage. The flux of particles from the bulk solution to the interface follows the theory of coagulation [42,52], which is given as follows:

$$J = -C \exp \frac{-V_B}{k_B T} \tag{1}$$

where V_B is the maximum energy value for the interaction potential and it also termed as the magnitude of the energy barrier. The constant C contains numerous experimental variables including the diffusion constant of particles (D), the particle concentration (C_B) and the curvature of the energy profile at V_B. It should be noted that C has various forms depending on different assumptions [52]; however, for all of them, C is constant as long as D and C_B remain constant. Therefore, the flux of the particles only depends on V_B; therefore, this is the focus.

2.2. DLVO Interaction

In order to compute the maximum energy barrier between a particle and a bubble, we consider the simplest yet most popular interaction: the DLVO theory [53,54]. This theory involves two interactions: the van der Waals (V_{VDW}) and electrostatic interaction (V_{EDL}). Note that we use a planar-spherical particle geometry because the size of mineral (a) is significantly smaller than that of a bubble. For this geometry, the V_{VDW} interaction at the separation distance between a plane and a sphere h is given as follows [55]:

$$\frac{V_{VDW}(h)}{k_B T} = -\frac{A_{132}\, a}{6h}\left[1 + \left(\frac{14h}{\lambda}\right)\right]^{-1} \tag{2}$$

where a is the colloid particle radius and λ is the characteristic wavelength of the interaction and 100 nm is the typical value used. In addition, A_{132} is the Hamaker constant for the interaction of particle 1 with bubble 2 in water 3. The A_{132} between particle and bubble in water can be approximately represented as [56]:

$$A_{132} = \left(\sqrt{A_{11}} - \sqrt{A_{33}}\right)\left(\sqrt{A_{22}} - \sqrt{A_{33}}\right) \tag{3}$$

The value of A_{22} can be acceptably considered as zero because the molecular density inside the bubble is too low compared with the liquid or solid phase [57]. Thus, A_{132} becomes

$$A_{132} = -\sqrt{A_{33}}\left(\sqrt{A_{11}} - \sqrt{A_{33}}\right) \tag{4}$$

Since A_{11} is typically larger than A_{33}, A_{132} becomes negative. Accordingly, the value of A_{132} employed in this paper is -3.21×10^{-21} J, which is representative value for a silica-bubble-water system [56]. As a consequence of this, V_{VDW} between the particle and the bubble in water tends to be positive, indicating that V_{VDW} becomes a repulsive interaction in the case of the particle-bubble system [57]. In addition, the V_{EDL} interaction for the planar-spherical geometry is described as follows [58]:

$$\frac{V_{EDL}(h)}{k_B T} = \pi \varepsilon_r \varepsilon_0 a\left[2\psi_p \psi_s \ln\left(\frac{1 + e^{-kh}}{1 - e^{-kh}}\right) + \left({\psi_p}^2 - {\psi_s}^2\right)\ln\left(1 - e^{-2kh}\right)\right] \tag{5}$$

$$\kappa = \frac{1}{l_d} = \left[\frac{2 I_s N_A 1000 e^2}{\varepsilon_r \varepsilon_0 k_B T}\right]^{1/2} \tag{6}$$

where $\varepsilon_r = \varepsilon/\varepsilon_0$ is the relative dielectric constant of the suspending liquid, ε is the dielectric constant of the suspending liquid, ε_0 is the permittivity of free space, ψ_p is the surface potential of the plate and ψ_s is the surface potential of the sphere. κ is the inverse of the electrical double layer thickness, which is known as the Debye–Huckel parameter: where I_s is the ionic strength, N_A is Avogadro's number, e is the elementary charge, k_B is the Boltzmann constant and T is the absolute temperature. Depending on

the parameter choices, the total interaction profile can be either favorable or unfavorable because they determine the magnitude of the energy barrier (E_B) [59,60]. The particle–bubble interactions have been routinely modeled using these two interactions [55,58].

2.3. Depletion Interaction

The simplest yet most powerful force is the depletion interaction because it enhances the attractive interactions between the particles and bubbles. The depletion interaction arises between large particles in a solution of relatively smaller non-adsorbing polymers, micelles, or smaller hard spheres. The basic effect is simple: when the separation distance of larger particles (h) is smaller than the diameter of the small particles, the small particles are excluded from the gap between the larger particles. This depletion of small particles between larger particles breaks the balance of osmotic pressure by the small particles, which results in inward pressure and this effectively functions as an attractive interaction [37,38,42]. Again, the bubble is significantly larger than the mineral particles and the depletion interaction (V_{DEP}) as a function of the separation distance between the large sphere (particle) and the planar wall (bubble) is given as follows [61]:

$$\begin{array}{ll} \frac{V_{DEP}(h)}{k_B T} & = -3\phi_p \frac{a}{R_g}\left(1-\frac{h}{2R_g}\right)^2 \quad , \quad (h < 2R_g) \\ & = 0 \quad , \quad (h \geq 2R_g) \end{array} \tag{7}$$

where ϕ_p is the volume fraction of the depletant and R_g is the radius of gyration of the depletants. It should be emphasized that this range of depletion interaction has a crucial function in determining the optimum conditions.

2.4. Steric Interaction

The polymers that are typically used for depletion attraction do not generally adhere to solid surfaces but they can be adsorbed at the air/water interface [62]. Polyethylene glycol (PEG), which is a typical depletion agent in aqueous systems, is surface active and lowers the air/water surface tension. In this situation, the polymers adsorbed at the bubble surface can function as a neutral polymer brush, which results in steric repulsive interactions between the solid particles that are to be adsorbed. This short-ranged repulsive interaction increases the E_B, thus hindering the particle attachment regardless of the existence of several attractive interactions. The efficiency of the steric interaction depends on the surface density σ (the number of molecules per area) and the initial brush thickness L_0. The steric interaction (V_{STE}) as a function of separation distance h is given, as follows [45,63,64]:

$$\begin{array}{ll} \frac{V_{STE}(h)}{k_B T} & = L_0 \sigma^{\frac{1}{2}}\left[\frac{7}{12}\left(\frac{h}{L_0}\right)^{-\frac{5}{4}} + \frac{5}{12}\left(\frac{h}{L_0}\right)^{\frac{7}{4}} - 1\right] \quad , \quad (h < L_0) \\ & = 0 \quad , \quad (h \geq L_0) \end{array} \tag{8}$$

2.5. Other Possible Interaction (Surface Coverage)

Numerous other possible interactions exist, as described in the introduction. One factor that could significantly influence the particle-bubble interaction is the surface coverage of the surfactant or particles [65,66]. When particles approach the bubble surface, the surfactant molecules or particles that already exist on the bubble surface restrict the other particles to be attached. In order to enable a successful attachment, a new free surface area must be created through compressing the existing particles to one side and thus the new particles can enter into the newly created area. The energy required to create a new free surface is related to the surface viscosity and elasticity [67–69]. In general, sufficient numbers of bubbles are formed and therefore the particle concentration at the bubble surface is typically low while the surfactant molecules (either collectors or frothers) always cover almost surface area of bubbles, which potentially hinders the attachment. Fortunately, simple surfactant molecules as collectors or frothers are, however, relatively easy to compress and expand to create an

unoccupied free surface. Furthermore, as demonstrated in the previous section, when the depletion agents are adsorbed on the bubble surface, the V_{STE} is significantly more dominant than this effect. Therefore, it is reasonable to neglect this effect a full stop and the final interaction energy in this article is as follows:

$$V_{TOT}(h) = V_{VDW}(h) + V_{EDL}(h) + V_{STE}(h) \quad (9)$$

3. Results and Discussion

3.1. Depletion Interaction with DLVO Interactions

First, two basic interactions are considered: electrostatic and van der Waals interactions. Figure 2 depicts the representative interaction energy profiles between a particle and a bubble using the parameters in Tables 1 and 2. It is clear that the EB of this interaction has an order of 10^3 k_BT, which cannot be overcome using thermal energy, k_BT. This high energy primarily arises from the size of the particles: particles with a typical size of 10–100 nm have an order of k_BT for similar electrostatic and van der Waals parameters in Tables 1 and 2, whereas particles with a size of ~10 μm have 10^3 k_BT due to their size. Nevertheless, when the depletant using parameters in Table 3 are considered, the attractive energy increases and lowers the E_B. In the case of a 20 mM monovalent salt concentration, the E_B decreases when the 10 wt % of depletant is added. It should be noted that V_{DEP} has a long range attractive interaction and the magnitude of V_{DEP} is comparable to V_{VDW}. This demonstrates that V_{DEP} could be the primary attractive interaction in the particle-bubble interaction.

In order to quantitatively understand the role of V_{DEP}, the interaction energy profiles with varying concentrations of depletion agent are described in Figure 2b. The DLVO interaction parameters are the same as those in Figure 2a. It is clearly seen that E_B decreases significantly with increases in the concentration of the depletion agent, which is also proven by our experimental results [70]. Therefore, this result strongly indicates that particle attachment could become far easier in the presence of depletion agents.

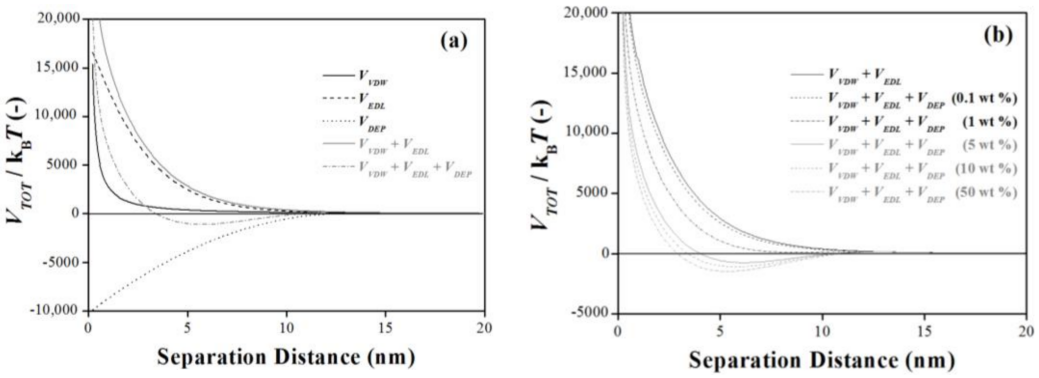

Figure 2. (**a**) The interaction energy profiles for the Derjaguin-Landau-Verwey-Overbeek (DLVO) with/without depletion attraction are represented as a function of separation distance h and (**b**) the energy profiles with varying concentrations of depletion reagent (0.1–50 wt %) are expressed as a function of the separation distance. The values of the silica-bubble-water Hamaker constant (-3.12×10^{-21} J), ionic strength (20 mM), silica surface potential (−0.02 V at pH 7), bubble surface potential (−0.025 V at pH 7), polymer radius of gyration (6.48×10^{-9} m) and polymer molecular weight (10^4 g/mol) are fixed.

Table 1. Parameter values of electrostatic interaction employed in the theoretical considerations.

Parameters	Values	References
Relative Permittivity, ε_r	78.5 [a]	
Permittivity of Free Space, ε_0	8.85×10^{-12} C^2/J m [a]	
Colloid Particle Radius, a	2.5×10^{-5} m [a]	
Sphere Surface Potential, Ψ_p	-0.02 V [a]	[71]
Plate Surface Potential, Ψ_s	-0.025 V [a]	[72]
Elementary Charge, e	1.60×10^{-19} C [a]	
Debye Length, l_d	2.15×10^{-9} m [a] 9.62×10^{-10}–9.62×10^{-9} m [b]	
Ionic Strength, I_S	2×10^{-2} mol/L [a] 10^{-3}–10^{-1} mol/L [b]	
Avogadro's Number, N_A	6.02×10^{23} 1/mol [a]	
Boltzman Constant, k_B	1.38×10^{-23} J/K [a]	
Absolute Temperature, T	298 K [a]	

[a] Figures 2–5 were expressed by these fixed parameter values as an electrostatic force. [b] Figure 5 was additionally represented with varying these parameter values as an electrostatic force to investigate the effect of ionic strengths and Debye length.

Table 2. Parameter values of van der Waals interaction employed in the theoretical considerations.

Parameters	Values	References
Hamaker Constant, A_{132}	-3.12×10^{-21} J [a]	[56]
Colloid Particle Radius, a	2.5×10^{-5} m [a]	
Directric Wavelength, λ	10^{-7} m [a]	
Boltzman Constant, k_B	1.38×10^{-23} J/K [a]	
Absolute Temperature, T	298 K [a]	

[a] Figures 2–5 were expressed by these fixed parameter values as a van der Waals force.

Table 3. Parameter values of depletion interaction employed in the theoretical considerations.

Parameter	Values	References
Polymer Radius of Gyration, R_g	6.48×10^{-9} m [a] 4.09×10^{-10}–2.58×10^{-8} m [c]	[73]
Polymer Volume Fraction, φ_p	8.84×10^{-1} [a] (−) 6.44×10^{-2}–9.86×10^{-1} [b] (−)	
Colloid Particle Radius, a	2.5×10^{-5} m [a]	
Polymer Weight Percent, Wt_p	10 wt % 0.1–50 wt % [b]	
Polymer Molecular Weight, MW	10^4 g/mol [a] 10^2–10^5 g/mol [c]	
Boltzman Constant, k_B	1.38×10^{-23} J/K [a]	
Absolute Temperature, T	298 K [a]	

[a] Figures 2–5 were expressed by these fixed parameter values as a depletion force. [b] Figure 2b was additionally represented with varying these parameter values as a depletion force to investigate the influence on the concentration of depletant. [c] Figure 4b was additionally represented with varying these parameter values as a depletion force to identify the influence on the radius of gyration and molecular weight of depletant.

3.2. Concentration Dependent: Surface Activity of Depletion Agents (Steric Effects)

Although the typical depletant in an aqueous system is a neutral polymer and weakly surface active, it can be adsorbed into the bubble or particle surface. Once adsorbed, those depletants at the surface function as polymer brushes rather than depletion agents [43–45,74]. Here, the depletion agent is assumed to be PEG because it is used in the companion experimental paper [70]. Assuming that PEG is reversibly adsorbed onto the bubble surface, which is an appropriate assumption for a soluble surfactant (i.e., Gibbs monolayer) [75], the surface concentration of the polymer depends on the bulk concentration of PEG in equilibrium, although most PEG molecules remain in the bulk [75,76]. Because

the depletion attraction and polymer brushes compete as their concentrations increase, an optimum concentration of depletion agent exists [70]. In general, a high concentration of depletant provides a higher attraction. However, if it is too high, then surface adsorption begins to occur, which prevents the attachment of particles into the bubbles.

Figure 3 presents the additional interaction energy profile through the modified DLVO prediction including the V_{DEP} and V_{STE} using the parameters listed in Tables 1–4. It can be seen that brush length becomes longer, the magnitudes of the V_{STE} gradually increases at the shorter range and thus it is hard for a particle to contact bubble despite the existence of the depletion force. In contrast, for brush lengths shorter, a weaker repulsive interaction is exhibited but they appear to have high energy barriers, which prove that the brush lowers the attachment probability. However, it should be noted that the magnitudes of the V_{STE} were overestimated for two reasons: first, non-ionic polymers such as PEG do not generally adhere to the particle (solid) surface [77], so the model for brushes on both sides are overestimated and second, the PEG on the bubble surface is mobile and compressible so that particles could create an empty surface through compressing the PEG at the bubble surface, thus enabling them to be adsorbed.

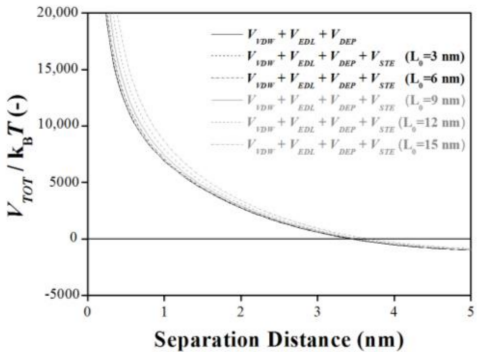

Figure 3. The interaction energy profiles for DLVO including the depletion and steric interaction are represented with variations in the brush thickness (3×10^{-9}–1.5×10^{-8} m) as a function of the separation. The values of the silica-bubble-water Hamaker constant (-3.12×10^{-21} J), ionic strengths (20 mM), silica surface potential (−0.02 V at pH 7), bubble surface potential (−0.025 V at pH 7), polymer weight (10 wt %), polymer volume fraction (8.84×10^{-1} (v/v)), polymer radius of gyration (6.48×10^{-9} m), polymer molecular weights (10^4 g/mol) and areal chain density (1 nm^{-2}) are fixed.

Table 4. Parameter values of steric interaction employed in the theoretical considerations.

Parameters	Values	References
Areal Chain Density, σ	1 nm^{-2} [a]	[78]
Brush Thickness, L_0	3×10^{-9}–1.5×10^{-8} m [b]	

[a] Figure 3 was expressed by these fixed parameter values as a steric force. [b] Figure 3 was additionally represented with varying these parameter values as a steric force to investigate the influence on the brush thickness.

3.3. Molecular Weight Dependence: How Is the Energy Barrier Lowered?

In this section, the effects of the molecular weights (MW) of the depletion agent are investigated. The interaction energy profiles were calculated with variations in the MW of the depletant from 10^2 to 10^5 g/mol and these are depicted in Figure 4. Overall, it was confirmed that there is a significant difference in the interaction energy profiles between the particles and bubbles depending on the changes in the MW of the depletant. In particular, the E_B gradually decreases as the MW of the depletant increases for low MW (10^2–10^3 g/mol), whereas it increased as the MW increased at high MW (10^3–10^5 g/mol). These trends are clearly seen in Figure 4a,b, respectively. This non-monotonic dependence results from the range of the depletion interaction depending on the MW because it is limited by the size of the depletion agents ($2R_g$). For a polymer in a good solvent such as PEG in

water, the radius of the gyration scales as $R_g \sim N^{0.6}$, where N is the degree of polymerization, which is proportional to MW [64]. The R_g values for 10^3 and 10^5 g/mol are 1.6 nm and 26 nm, respectively.

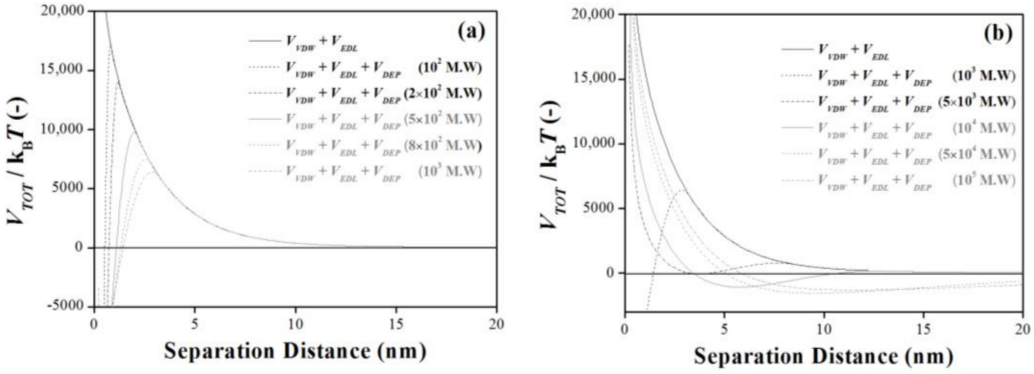

Figure 4. The interaction energy profiles for DLVO including the depletion interaction with varying the lower molecular weight of the depletant (10^2–10^3 MW) (**a**) and higher molecular weight of the depletant (10^3–10^5 MW) (**b**) are represented as a function of the separation distance, respectively. The values of the silica-bubble-water Hamaker constant (-3.12×10^{-21} J), ionic strength (20 mM), silica surface potential (−0.02 V at pH 7), bubble surface potential (−0.025 V at pH 7), polymer weight (10 wt %) and polymer volume fraction (8.84×10^{-1} (v/v)) are fixed.

This depletion range competes with the electrostatic interaction range, which is approximately the Debye length (l_d). That is, for the depletion attraction to lower the E_B, the range of the V_{DEP} should be greater than that of the V_{EDL} and thus a larger MW depletant is more effective. However, it is not always effective because a large MW depletant provides a lower osmotic pressure: from $|V_{DEP}| \sim \varphi_p a/R_g \sim naR_g^2$, V_{DEP} is proportional to the number of molecules and for two solutions with the same mass fraction of depletant solution, the low MW solution has significantly more depletant molecules compared with the high MW solution. In principal, the concentration of high MW depletant could be increased to be considerably high but the viscosity of the solution also increases rapidly [79], thus resulting in the flotation becoming practically impossible.

3.4. Ionic Strength Dependent: How Is the Energy Barrier Lowered?

As described above, the ionic strength changes the Debye length, thereby controlling the range of the repulsive interactions. In order to verify the effect of the ionic strength, the interaction energy profiles were also calculated using the classical DLVO predictions (a) and modified DLVO predictions including depletion force (b) with variations in the ionic strengths (10^{-3}–10^{-1} M) and these are described in Figure 5, respectively. As expected, the ionic strengths decreased the magnitudes of E_B between the particle and bubble with increases in the ionic strengths. In particular, as illustrated in Figure 5b, E_B decreased more rapidly as the ionic strength increased in the presence of 10 wt % of 10^4 g/mol PEG, which corresponds to 6.5 nm in radius. The depletant does not lower the E_B for lower ionic strengths for $l_d > R_g$. As the ionic strength increased or l_d decreased and approached R_g (6.5 nm for 10^4 g/mol), the difference became more significant, exhibiting a greater difference of E_B. For comparison, l_d is ~2.15 nm for 20 mM.

The EB is determined through the interplay between the range of attraction and repulsion. The long attraction range of the depletion attraction results in a significant effect on the E_B. Specially, for certain conditions (10 wt % of 10^4 g/mol PEG with $> 2 \times 10^{-2}$ M of ionic strength), the particle-bubble interaction becomes more attractive; thus, particles could be easily adsorbed onto the bubble surface. Considering the magnitudes of E_B using classical and modified DLVO predictions for ionic strengths, the V_{DEP} more significantly affects the interaction force between the particle and bubble when $l_d < R_g$. It should be noted that the dissolved ions could also function as depletants but both the range and the

magnitude of the interaction were significantly smaller than the effect of PEG because $|V_{DEP}| \sim R_g^2$ and this is approximately 100 times smaller and the range is only an order of 0.1 nm.

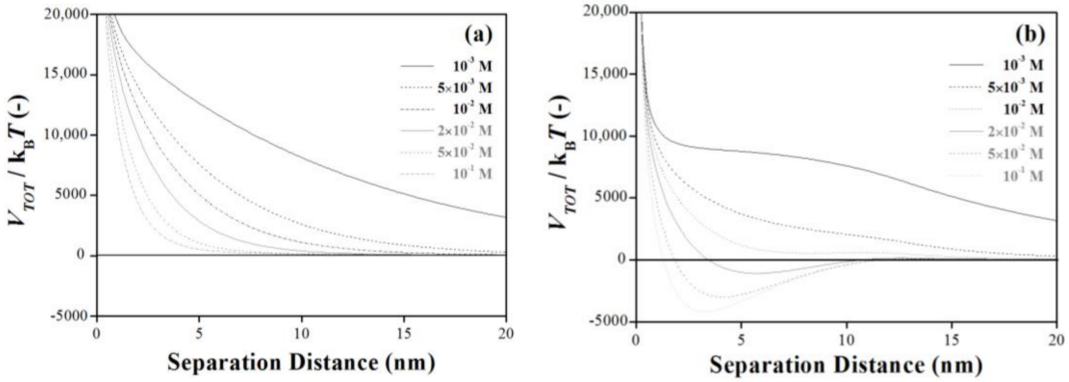

Figure 5. The interaction energy profiles for classical DLVO (**a**) and modified-DLVO including the depletion interaction (**b**) with variations in the ionic strengths (10^{-3}–10^{-1} M) are represented as a function of the separation distance, respectively. The values of the silica-bubble-water Hamaker constant (-3.12×10^{-21} J), silica surface potential (−0.02 V at pH 7), bubble surface potential (−0.025 V at pH 7), polymer weight (10 wt %), polymer volume fraction (8.84×10^{-1} (v/v)), polymer radius of gyration (6.48×10^{-9} m) and polymer molecular weights (10^4 g/mol) are fixed.

3.5. Concentration Dependent: Gravity Versus Depletion (Particle Size Dependent)

Once the particles are attached at the bubble surface, the interaction energy profile that is considered above becomes trivial because it is now governed by another force, that is, the capillary force [80]. This force could be sufficiently strong that the particles cannot escape the interface except in two situations: (1) either completely hydrophilic or hydrophobic particles that have a tiny capillary force and (2) nanoparticles that have a lower capillary interaction. When a single spherical particle of a radius a is immersed to its equilibrium depth in a planar gas–water interface, this depth is $a(1 - \cos\theta)$, where θ is the contact angle of the bubble-water interface. Neglecting the external forces (e.g., gravity), with water–solid (γ_{ws}) and water–gas (γ_{gw}) interfacial tension, the capillary energy (i.e., capillary interaction) is computed as follows [80]:

$$V_{CAP} = -\pi a^2 \gamma_{gw} (1 - \cos\theta)^2 \quad (10)$$

According to the literature, the magnitude of this capillary interaction is in the order of $>10^6$ J for a micron-sized particle with moderate hydrophobicity [81,82]. Likewise, the capillary force significantly affects the flotation system (i.e., solid–gas system), maintaining particles at the interface while floating.

However, the depletion attraction could hold the particles at the interface without this capillary energy. Assuming that the gravity due to the weight of the particles is the only reason to escape from the interface and considering that the particles are already attached to the interface by the depletion attraction, it is natural for particles to tend to escape from the interface via gravitational force. As soon as the particles escape from the interface, the depletion force is exerted on the particle to move it back into the interface. This gravitational force of the particle $4\rho g\pi r^3/3$ is balanced with the depletion force ($-\partial V_{DEP}/\partial h$). Applying the 10 wt % of 10^4 g/mol PEG solution as in Figure 1, the depletion force is computed through taking the derivative of the depletion energy in Equation (7). The maximum particle size that the depletion force can hold at the interface is ~10 μm. Because the capillary force is almost always present, the depletion force can maintain a larger particle size [80]. It should be noted that the capillary forces are typically far greater than the depletion force, except for the cases that the particles are nearly hydrophilic.

4. Conclusions

Throughout this article, we have theoretically explored the role of the depletion interaction in particle-bubble interactions, which might be very crucial in flotation techniques. Using the common DLVO theory, which is considered to describe the main interactions between particles and bubbles, we examined how the depletion interaction changes the magnitude of the E_B when many experimental variables such as the ionic strength and molecular weight of the depletion agent are varied. These E_B decreases determine the overall flotation efficiency: a lower energy barrier leads to a high attachment probability of particles, thus leading to superb floatability. Interestingly, additional depletion agents could worsen the flotation process if the concentration becomes too high. The depletion agents dispersed in the solution could also be adsorbed into the bubble surface and these adsorbed agents might function as polymer brushes, thereby yielding a strong steric repulsion. This implies that there is an optimum concentration of depletion agents: high concentrations of depletion agents increase the attachment probability while it could adversely affect the flotation process through developing repulsive steric interactions as polymeric brushes. In addition, it was found that the competition of the two length scales is a crucial factor in effectively decreasing the energy barrier. The first length scale is the Debye length, which represents a repulsive interaction and the second length scale is the gyration radius of the depletion agents, which reflects the range of attractive interaction. This indicates that optimum molecular weights exist for the depletion agents and the salt concentration.

Determining the optimum concentration and molecular weight of the depletion agents involves numerous interaction parameters including the Hamaker constant, surface charge density of particles, ionic strength and particle size. These parameters differ considerably depending on the types of particle and processes, for which particular strategies might be required. However, the central theme in this paper remains unchanged: an optimum concentration and molecular weight exist for any system. These conditions can be found experimentally: the Debye length can be determined through ionic strength, thereby enabling the optimum molecular weight to be selected; the optimum concentration can be easily determined through measuring the surface tension of the bubbles because it represents how much the polymer molecules are adsorbed in the surface.

In principle, this strategy could be applied to mixed particle systems consisting of two or more species. Suppose that there are two different types of particles and they exhibit different surface properties, one of which has more negative charges on the surface than the other. Through accurately controlling the attractive interaction using depletion interaction, a "sweet spot" could be found to decrease the E_B significantly for one type but not for the other type. Although it is uncertain how difficult it would be to find this "sweet spot," we could intentionally design this type of environment in order to obtain the right conditions.

Some important interactions that have been ignored, such as hydrophobic interactions, would also have a significant influence on the particle–bubble interaction with/without the depletion attraction. The influence of hydrophobic attraction on the bubble–particle interaction with the depletion attraction cannot be simply estimated at this stage because it will highly depend on the type of materials for separation: hydrophobic versus hydrophobic, hydrophobic versus hydrophilic, or hydrophilic versus hydrophilic. Moreover, vigorous fluid flows could significantly alter the particle–bubble interactions and it remains largely unknown how much the fluid flow affects the particle–bubble interactions in the presence of depletion agents. These questions remain as future research.

Author Contributions: J.C. and S.Q.C. compiled the information and wrote the manuscript; G.K., S.C., K.K. and Y.H. collaborated in the edition of the manuscript; S.A.B. reviewed the manuscript and gave feedback for improvement; and, H.K. assisted in all of the aforementioned activities as academic supervisor.

Funding: This research was funded by the Basic Science Research Program through the National Research Foundation of Korea (NRF-2012R1A6A3A040395) and the Korea Energy and Mineral Resources Engineering Program (KEMREP).

Conflicts of Interest: The authors declare no conflict of interest.

References

1. Fuerstenau, M.; Jameson, G.; Yoon, R.-H. *Froth Flotation: A Century of Innovation*; SME: Littleton, CO, USA, 2007.
2. Choi, J.; Park, K.; Hong, J.; Park, J.; Kim, H. Arsenic removal from mine tailings for recycling via flotation. *Mater. Trans.* **2013**, *54*, 2291–2296. [CrossRef]
3. Park, K.; Choi, J.; Gomez-Flores, A.; Kim, H. Flotation behavior of arsenopyrite and pyrite and their selective separation. *Mater. Trans.* **2015**, *56*, 435–440. [CrossRef]
4. Park, K.; Park, S.; Choi, J.; Kim, G.; Tong, M.P.; Kim, H. Influence of excess sulfide ions on the malachite-bubble interaction in the presence of thiol-collector. *Sep. Purif. Technol.* **2016**, *168*, 1–7. [CrossRef]
5. Choi, J.; Kim, W.; Chae, W.; Kim, S.B.; Kim, H. Electrostatically controlled enrichment of lepidolite via flotation. *Mater. Trans.* **2012**, *53*, 2191–2194. [CrossRef]
6. Choi, J.; Choi, S.Q.; Park, K.; Han, Y.; Kim, H. Flotation behavior of malachite in mono- and di-valent salt solutions using sodium oleate as a collector. *Int. J. Miner. Process.* **2016**, *146*, 38–45. [CrossRef]
7. Xing, Y.W.; Gui, X.H.; Cao, Y.J.; Wang, Y.W.; Xu, M.D.; Wang, D.Y.; Li, C.W. Effect of compound collector and blending frother on froth stability and flotation performance of oxidized coal. *Powder Technol.* **2017**, *305*, 166–173. [CrossRef]
8. Espiritu, E.R.L.; da Silva, G.R.; Azizi, D.; Larachi, F.; Waters, K.E. The effect of dissolved mineral species on bastnäsite, monazite and dolomite flotation using benzohydroxamate collector. *Colloids Surf. A-Physicochem. Eng. Asp.* **2018**, *539*, 319–334. [CrossRef]
9. Schubert, H.; Bischofberger, C. On the hydrodynamics of flotation machines. *Int. J. Miner. Process.* **1978**, *5*, 131–142. [CrossRef]
10. Schubert, H. On the turbulence-controlled microprocesses in flotation machines. *Int. J. Miner. Process.* **1999**, *56*, 257–276. [CrossRef]
11. Safari, M.; Deglon, D. An attachment-detachment kinetic model for the effect of energy input on flotation. *Miner. Eng.* **2018**, *117*, 8–13. [CrossRef]
12. Nguyen, A.V.; Nalaskowski, J.; Miller, J.D. A study of bubble-particle interaction using atomic force microscopy. *Miner. Eng.* **2003**, *16*, 1173–1181. [CrossRef]
13. Hoseinian, F.S.; Rezai, B.; Kowsari, E. The main factors effecting the efficiency of Zn(II) flotation: Optimum conditions and separation mechanism. *J. Environ. Manag.* **2018**, *207*, 169–179. [CrossRef] [PubMed]
14. Pan, L.; Jung, S.; Yoon, R.H. A fundamental study on the role of collector in the kinetics of bubble-particle interaction. *Int. J. Miner. Process.* **2012**, *106*, 37–41. [CrossRef]
15. Hong, G.; Choi, J.; Han, Y.; Yoo, K.S.; Kim, K.; Kim, S.B.; Kim, H. Relationship between surface characteristics and floatability in representative sulfide minerals: Role of surface oxidation. *Mater. Trans.* **2017**, *58*, 1069–1075. [CrossRef]
16. Phan, C.M.; Nguyen, A.V.; Miller, J.D.; Evans, G.M.; Jameson, G.J. Investigations of bubble-particle interactions. *Int. J. Miner. Process.* **2003**, *72*, 239–254. [CrossRef]
17. Ralston, J.; Fornasiero, D.; Hayes, R. Bubble-particle attachment and detachment in flotation. *Int. J. Miner. Process.* **1999**, *56*, 133–164. [CrossRef]
18. Verrelli, D.I.; Koh, P.T.L.; Nguyen, A.V. Particle-bubble interaction and attachment in flotation. *Chem. Eng. Sci.* **2011**, *66*, 5910–5921. [CrossRef]
19. Kouachi, S.; Hassas, B.V.; Hassanzadeh, A.; Celik, M.S.; Bouhenguel, M. Effect of negative inertial forces on bubble-particle collision via implementation of schulze collision efficiency in general flotation rate constant equation. *Colloids Surf. A-Physicochem. Eng. Asp.* **2017**, *517*, 72–83. [CrossRef]
20. Corin, K.C.; Reddy, A.; Miyen, L.; Wiese, J.G.; Harris, P.J. The effect of ionic strength of plant water on valuable mineral and gangue recovery in a platinum bearing ore from the merensky reef. *Miner. Eng.* **2011**, *24*, 131–137. [CrossRef]
21. Ejtemaei, M.; Irannajad, M.; Gharabaghi, M. Influence of important factors on flotation of zinc oxide mineral using cationic, anionic and mixed (cationic/anionic) collectors. *Miner. Eng.* **2011**, *24*, 1402–1408. [CrossRef]
22. Hu, Y.H.; Chen, P.; Sun, W. Study on quantitative structure-activity relationship of quaternary ammonium salt collectors for bauxite reverse flotation. *Miner. Eng.* **2012**, *26*, 24–33. [CrossRef]

23. Jiang, H.; Sun, Z.C.; Xu, L.H.; Hu, Y.H.; Huang, K.; Zhu, S.S. A comparison study of the flotation and adsorption behaviors of diaspore and kaolinite with quaternary ammonium collectors. *Miner. Eng.* **2014**, *65*, 124–129. [CrossRef]
24. Parker, G.K.; Buckley, A.N.; Woods, R.; Hope, G.A. The interaction of the flotation reagent, *n*-octanohydroxamate, with sulfide minerals. *Miner. Eng.* **2012**, *36–38*, 81–90. [CrossRef]
25. Peng, Y.; Seaman, D. The flotation of slime-fine fractions of Mt. Keith pentlandite ore in de-ionised and saline water. *Miner. Eng.* **2011**, *24*, 479–481. [CrossRef]
26. Shackleton, N.J.; Malysiak, V.; De Vaux, D.; Plint, N. Water quality—A comparative study between moncheite and pentlandite in mixture with pyroxene. *Miner. Eng.* **2012**, *36–38*, 53–64. [CrossRef]
27. Vidyadhar, A.; Kumari, N.; Bhagat, R.P. Adsorption mechanism of mixed collector systems on hematite flotation. *Miner. Eng.* **2012**, *26*, 102–104. [CrossRef]
28. Wang, B.; Peng, Y.J. The effect of saline water on mineral flotation—A critical review. *Miner. Eng.* **2014**, *66–68*, 13–24. [CrossRef]
29. Zhang, M.; Peng, Y.J.; Xu, N. The effect of sea water on copper and gold flotation in the presence of bentonite. *Miner. Eng.* **2015**, *77*, 93–98. [CrossRef]
30. Choi, J.; Lee, E.; Choi, S.Q.; Lee, S.; Han, Y.; Kim, H. Arsenic removal from contaminated soils for recycling via oil agglomerate flotation. *Chem. Eng. J.* **2016**, *285*, 207–217. [CrossRef]
31. Kim, G.; Park, K.; Choi, J.; Gomez-Flores, A.; Han, Y.; Choi, S.Q.; Kim, H. Bioflotation of malachite using different growth phases of *Rhodococcus opacus*: Effect of bacterial shape on detachment by shear flow. *Int. J. Miner. Process.* **2015**, *143*, 98–104. [CrossRef]
32. Kim, G.; Choi, J.; Silva, R.A.; Song, Y.; Kim, H. Feasibility of bench-scale selective bioflotation of copper oxide minerals using rhodococcus opacus. *Hydrometallurgy* **2017**, *168*, 94–102. [CrossRef]
33. Liu, W.Y.; Moran, C.J.; Vink, S. A review of the effect of water quality on flotation. *Miner. Eng.* **2013**, *53*, 91–100. [CrossRef]
34. Kim, H.N.; Walker, S.L. *Escherichia coli* transport in porous media: Influence of cell strain, solution chemistry and temperature. *Colloids Surf. B-Biointerfaces* **2009**, *71*, 160–167. [CrossRef] [PubMed]
35. Fielden, M.L.; Hayes, R.A.; Ralston, J. Surface and capillary forces affecting air bubble-particle interactions in aqueous electrolyte. *Langmuir* **1996**, *12*, 3721–3727. [CrossRef]
36. Nguyen, A.V.; Schulze, H.J.; Ralston, J. Elementary steps in particle-bubble attachment. *Int. J. Miner. Process.* **1997**, *51*, 183–195. [CrossRef]
37. Asakura, S.; Oosawa, F. Interaction between particles suspended in solutions of macromolecules. *J. Polym. Sci.* **1958**, *33*, 183–192. [CrossRef]
38. Mao, Y.; Cates, M.E.; Lekkerkerker, H.N.W. Depletion force in colloidal systems. *Physica A* **1995**, *222*, 10–24. [CrossRef]
39. Walz, J.Y.; Sharma, A. Effect of long range interactions on the depletion force between colloidal particles. *J. Colloid Interface Sci.* **1994**, *168*, 485–496. [CrossRef]
40. Lekkerkerker, H.N.W.; Tuinier, R. *Colloids and the Depletion Interaction*; Springer: Dordrecht, The Netherlands, 2011.
41. Kim, K.; Kim, S.; Ryu, J.; Jeon, J.; Jang, S.G.; Kim, H.; Gweon, D.G.; Im, W.B.; Han, Y.; Kim, H.; et al. Processable high internal phase pickering emulsions using depletion attraction. *Nat. Commun.* **2017**, *8*, 14305. [CrossRef] [PubMed]
42. Zasadzinski, J.A.; Alig, T.F.; Alonso, C.; de la Serna, J.B.; Perez-Gil, J.; Taeusch, H.W. Inhibition of pulmonary surfactant adsorption by serum and the mechanisms of reversal by hydrophilic polymers: Theory. *Biophys. J.* **2005**, *89*, 1621–1629. [CrossRef] [PubMed]
43. Biggs, S. Steric and bridging forces between surfaces fearing adsorbed polymer: An atomic-force microscopy study. *Langmuir* **1995**, *11*, 156–162. [CrossRef]
44. Gotchev, G.; Kolarov, T.; Khristov, K.; Exerowa, D. Electrostatic and steric interactions in oil-in-water emulsion films from pluronic surfactants. *Adv. Colloid Interface Sci.* **2011**, *168*, 79–84. [CrossRef] [PubMed]
45. Kim, J.U.; Matsen, M.W. Repulsion exerted on a spherical particle by a polymer brush. *Macromolecules* **2008**, *41*, 246–252. [CrossRef]
46. Han, P.; Wang, X.T.; Cai, L.; Tong, M.P.; Kim, H. Transport and retention behaviors of titanium dioxide nanoparticles in iron oxide-coated quartz sand: Effects of pH, ionic strength and humic acid. *Colloids Surf. A-Physicochem. Eng. Asp.* **2014**, *454*, 119–127. [CrossRef]

47. Han, Y.; Hwang, G.; Park, S.; Gomez-Flores, A.; Jo, E.; Eom, I.C.; Tong, M.P.; Kim, H.J.; Kim, H. Stability of carboxyl-functionalized carbon black nanoparticles: The role of solution chemistry and humic acid. *Environ. Sci. Nano* **2017**, *4*, 800–810. [CrossRef]
48. Jiang, X.J.; Tong, M.P.; Kim, H. Influence of natural organic matter on the transport and deposition of zinc oxide nanoparticles in saturated porous media. *J Colloid Interface Sci.* **2012**, *386*, 34–43. [CrossRef] [PubMed]
49. Kim, H.N.; Bradford, S.A.; Walker, S.L. *Escherichia coli* O157:H7 transport in saturated porous media: Role of solution chemistry and surface macromolecules. *Environ. Sci. Technol.* **2009**, *43*, 4340–4347. [CrossRef] [PubMed]
50. Abrahamson, J. Collision rates of small particles in a vigorously turbulent fluid. *Chem. Eng. Sci.* **1975**, *30*, 1371–1379. [CrossRef]
51. Schubert, H. On the optimization of hydrodynamics in fine particle flotation. *Miner. Eng.* **2008**, *21*, 930–936. [CrossRef]
52. Hiemenz, P.C. *Principles of Colloid and Surface Chemistry*, 2nd ed.; M. Dekker: New York, NY, USA, 1986.
53. Derjaguin, B.; Landau, L. Theory of the stability of strongly charged lyophobic sols and of the adhesion of strongly charged-particles in solutions of electrolytes. *Prog. Surf. Sci.* **1941**, *14*, 633–662. [CrossRef]
54. Verwey, E.J.W.; Nes, K.V.; Overbeek, J.T.G. *Theory of the Stability of Lyophobic Colloids: The Interaction of Sol Particles Having an Electric Double Layer*; Elsevier: New York, NY, USA, 1948.
55. Gregory, J. Approximate expressions for retarded vanderwaals interaction. *J. Colloid Interface Sci.* **1981**, *83*, 138–145. [CrossRef]
56. Yoon, R.H. The role of hydrodynamic and surface forces in bubble-particle interaction. *Int. J. Miner. Process.* **2000**, *58*, 129–143. [CrossRef]
57. Lu, S. Hydrophobic interaction in flocculation and flotation 3. Role of hydrophobic interaction in particle-bubble attachment. *Colloid Surf.* **1991**, *57*, 73–81. [CrossRef]
58. Chrysikopoulos, C.V.; Syngouna, V.I. Attachment of bacteriophages MS2 and ΦX174 onto kaolinite and montmorillonite: Extended-DLVO interactions. *Colloids Surface. B Biointerfaces* **2012**, *92*, 74–83. [CrossRef] [PubMed]
59. Kim, H.N.; Walker, S.L.; Bradford, S.A. Macromolecule mediated transport and retention of *Escherichia coli* O157:H7 in saturated porous media. *Water Res.* **2010**, *44*, 1082–1093. [CrossRef] [PubMed]
60. Han, Y.; Hwang, G.; Kim, D.; Bradford, S.A.; Lee, B.; Eom, I.; Kim, P.J.; Choi, S.Q.; Kim, H. Transport, retention and long-term release behavior of ZnO nanoparticle aggregates in saturated quartz sand: Role of solution pH and biofilm coating. *Water Res.* **2016**, *90*, 247–257. [CrossRef] [PubMed]
61. Bickel, T. Depletion forces near a soft surface. *J. Chem. Phys.* **2003**, *118*, 8960–8968. [CrossRef]
62. Reed, K.M.; Borovicka, J.; Horozov, T.S.; Paunov, V.N.; Thompson, K.L.; Walsh, A.; Armes, S.P. Adsorption of sterically stabilized latex particles at liquid surfaces: Effects of steric stabilizer surface coverage, particle size and chain length on particle wettability. *Langmuir* **2012**, *28*, 7291–7298. [CrossRef] [PubMed]
63. Alexander, S. Adsorption of chain molecules with a polar head a-scaling description. *J. Phys.* **1977**, *38*, 983–987. [CrossRef]
64. Degennes, P.G. Polymers at an interface; a simplified view. *Adv. Colloid Interface Sci.* **1987**, *27*, 189–209. [CrossRef]
65. Helgason, T.; Awad, T.S.; Kristbergsson, K.; McClements, D.J.; Weiss, J. Effect of surfactant surface coverage on formation of solid lipid nanoparticles (SLN). *J. Colloid Interface Sci.* **2009**, *334*, 75–81. [CrossRef] [PubMed]
66. Lin, S.-Y.; Tsay, R.-Y.; Lin, L.-W.; Chen, S.-I. Adsorption kinetics of $C_{12}E_8$ at the air-water interface: Adsorption onto a clean interface. *Langmuir* **1996**, *12*, 6530–6536. [CrossRef]
67. Choi, S.Q.; Steltenkamp, S.; Zasadzinski, J.A.; Squires, T.M. Active microrheology and simultaneous visualization of sheared phospholipid monolayers. *Nat. Commun.* **2011**, *2*, 312. [CrossRef] [PubMed]
68. Leal-Calderon, F.; Schmitt, V. Solid-stabilized emulsions. *Curr. Opin. Colloid Interface Sci.* **2008**, *13*, 217–227. [CrossRef]
69. Stocco, A.; Rio, E.; Binks, B.P.; Langevin, D. Aqueous foams stabilized solely by particles. *Soft Matter* **2011**, *7*, 1260–1267. [CrossRef]
70. Kim, G.; Choi, J.; Choi, S.; Kim, K.; Han, Y.; Bradford, S.A.; Choi, S.Q.; Kim, H. Application of depletion attraction in mineral flotation: II. Effects of depletant concentration. *Minerals* **2018**, under review.
71. Castro, S.H.; Baltierra, L. Study of the surface properties of enargite as a function of pH. *Int. J. Miner. Process.* **2005**, *77*, 104–115. [CrossRef]

72. Elmallidy, A.M.; Mirnezami, M.; Finch, J.A. Zeta potential of air bubbles in presence of frothers. *Int. J. Miner. Process.* **2008**, *89*, 40–43.
73. Ling, K.; Jiang, H.Y.; Zhang, Q.Q. A colorimetric method for the molecular weight determination of polyethylene glycol using gold nanoparticles. *Nanoscale Res. Lett.* **2013**, *8*, 538. [CrossRef] [PubMed]
74. Gast, A.P.; Leibler, L. Interactions of sterically stabilized particles suspended in a polymer-solution. *Macromolecules* **1986**, *19*, 686–691. [CrossRef]
75. Israelachvili, J.N. *Intermolecular and Surface Forces*, 3rd ed.; Academic Press: Cambridge, MA, USA, 2011.
76. Needham, D.; Kim, D.H. Peg-covered lipid surfaces: Bilayers and monolayers. *Colloids Surf. B Biointerfaces* **2000**, *18*, 183–195. [CrossRef]
77. Herrmann, A.; Clague, M.J.; Blumenthal, R. Enhancement of viral fusion by nonadsorbing polymers. *Biophys. J.* **1993**, *65*, 528–534. [CrossRef]
78. Unsworth, L.D.; Sheardown, H.; Brash, J.L. Protein-resistant poly(ethylene oxide)-grafted surfaces: Chain density-dependent multiple mechanisms of action. *Langmuir* **2008**, *24*, 1924–1929. [CrossRef] [PubMed]
79. Gonzaleztello, P.; Camacho, F.; Blazquez, G. Density and viscosity of concentrated aqueous-solutions of polyethylene-glycol. *J. Chem. Eng. Data* **1994**, *39*, 611–614. [CrossRef]
80. Levine, S.; Bowen, B.D.; Partridge, S.J. Stabilization of emulsions by fine particles I. Partitioning of particles between continuous phase and oil/water interface. *Colloid Surf.* **1989**, *38*, 325–343. [CrossRef]
81. Binks, B.P.; Horozov, T. *Colloidal Particles at Liquid Interfaces*; Cambridge University Press: Cambridge, UK, 2006.
82. Kim, K.; Park, K.; Kim, G.; Kim, H.; Choi, M.C.; Choi, S.Q. Surface charge regulation of carboxyl terminated polystyrene latex particles and their interactions at the oil/water interface. *Langmuir* **2014**, *30*, 12164–12170. [CrossRef] [PubMed]